Constraints on the dark Z model from Higgs boson phenomenology

Dong-Won Jung[‡]

Department of Physics, Yonsei University, Seoul 03722, Korea and
Department of Physics, Chonnam National University, Gwangju 61186, Korea

Kang Young Lee[*] and Chaehyun Yu[†]

Department of Physics Education and RINS, Gyeongsang National University, Jinju 52828, Korea

We consider the phenomenology of the Higgs bosons in the hidden sector model mediated by an additional SU(2) scalar doublet. With the mediator scalar doublet, the Higgs sector of the model is extended to be that of the two Higgs doublet model of type I. The mediator scalar doublet is connected to the hidden sector with the hidden $U(1)_X$ gauge charge. Then the $U(1)_X$ gauge symmetry is spontaneously broken by the electroweak symmetry breaking and the hidden U(1) gauge boson gets the mass to give rise to a dark Z boson. Using the programs HiggsBounds and HiggsSignals, we incorporate current experimental limits from LEP, Tevatron, and LHC to examine the Higgs sector in our model and derive constraints on model parameters together with the electroweak processes. As a result, our model favors the light dark Z boson. We also investigate the implications of the model on the dark matter phenomenology when the hidden fermion is a dark matter candidate.

I. INTRODUCTION

Following the discovery of the Higgs boson [1,2], extensive study on the scalar sector has been conducted to reveal the detailed properties of the Higgs boson at the Large Hadron Collider (LHC). Although the Higgs mechanism with a $SU(2)_L$ doublet Higgs field provides a tenable explanation of the electroweak symmetry breaking (EWSB) in the Standard Model (SM), there still exist many theoretical drawbacks, such as the naturalness problem, flavor structure, and origin of neutrino masses related to the Higgs sector. Therefore, many new physics models beyond the SM suggest extensions of the Higgs sector. So far, no significant deviations from the SM are shown in experiments and the precise measurements of Higgs boson sectors provide strong constraints on the theoretical structure of new physics (NP).

It is another shortcoming of the SM that the SM does not include the dark matter (DM) candidates of the Universe, which are demanded for explanation of the present astrophysical and cosmological observations. Various kinds of DM candidates have emerged from theoretical models beyond the SM as natural ingredients of the models [3]. Meanwhile we can consider another type of DM candidate, which is very weakly interacting with the SM sector and included in the "hidden" sector.

The phenomenology of DM in the hidden sector strongly depends on how to connect to the SM fields. Recently, we have suggested a hidden sector model where a SM singlet fermion is a DM candidate and an additional Higgs doublet mediates between the hidden sector and the SM sector [4]. A hidden $U(1)_X$ gauge symmetry is introduced and the $U(1)_X$ charge is assigned to the hidden sector fermion and the mediator Higgs doublet for the mediator to couple to the hidden sector. Then the $U(1)_X$ gauge symmetry is spontaneously broken by the EWSB in this model. Thus, there exists an extra massive gauge boson mixed with the SM Z boson as a result. We call it a dark Z boson, which is dubbed Z', since its couplings to the SM fermions are proportional to those of the ordinary Z boson with the suppression factor of the mixing angle. The dark Z boson mass is of order the electroweak scale at most and could be much lighter. The light Z' boson affects the electroweak processes and is stringently constrained by the collider and the low energy neutral current (NC) experiments [4,5]. Massive dark gauge bosons have also been considered in the literature [6].

Since we introduce one more Higgs doublet as the mediator field, there are two SU(2) Higgs doublets in the

[*]Corresponding author: kylee.phys@gnu.ac.kr
[†]Corresponding author: chyu@kias.re.kr
[‡]dongwon.jung@yonsei.ac.kr

model and the Higgs sector is the same as the two Higgs doublet model (2HDM). Because of the $U(1)_X$ charge, the additional Higgs doublet does not couple to the SM fermions and, consequently, the Higgs contents are comparable to the 2HDM of type I. The discrete symmetry in the typical 2HDM is absent in the model and the Yukawa structure is controlled by the $U(1)_X$ gauge symmetry as in Ref. [7].

After EWSB, there exist three additional Higgs bosons, one CP-even neutral Higgs boson and a pair of charged Higgs bosons. Note that no CP-odd neutral Higgs boson appears in this model since corresponding degree of freedom is accountable for the dark Z boson mass. It is one of the distinctive features of this model. In this paper we carry out an intensive study on the model with the phenomenology of Higgs bosons and the electroweak processes. The electroweak processes depend on the dark Z mass and mixing angle principally. The model parameters in the Higgs sector are two masses of neutral and charged Higgs bosons, m_h and $m_\pm$, and two mixing angles α and β for them, respectively, in addition to the dark Z mass and mixing. We probe the consistency of these parameters with a large number of experimental data using the public codes HiggsBounds [8] and HiggsSignals [9]. The former provides the 95% exclusion limit for the extra scalar production in collider experiments, while the latter provides χ^2 and P values of a model with respect to observables of the SM-like Higgs boson at the LHC.

We also show that our minimal hidden sector is valid for the present DM phenomenology. We assume the DM candidate is a Dirac fermion. The $U(1)_X$ charge of the DM fermion is independent of the visible sector. The interaction strength of the DM fermion to the Z' and the DM mass are new free parameters to adjust the observed relic density and the discovery limit for the DM-nucleon cross sections. The dark Z boson is a portal to the hidden sector where DM is living. With a comprehensive numerical analysis, we show that a significant portion of the parameter space can explain the known DM properties in relation to cosmology and astrophysics. We also provide arguments about the validity of the results considering astrophysical phenomena such as supernova cooling.

This paper is organized as follows. The model is explained in Sec. II. In Sec. III we analyze this model mainly focusing on the Higgs sector. We describe the analysis of the phenomenology of the Higgs bosons with HiggsBounds and HiggsSignals in Sec. III A. Discussion about constraints on the model parameters together with the electroweak processes, atomic parity violation, ρ parameter, and Z boson total width follows in Secs. III B, III C, and III D, respectively. We show that our dark matter candidate is acceptable for the relic density of the Universe and the present direct detection experiments in Sec. IV. Section V is devoted to the summary of the results and conclusion.

II. THE MODEL

We assume that the hidden sector consists of a Dirac fermion with $U(1)_X$ gauge symmetry. The hidden sector fermion is a SM gauge singlet and the dark matter candidate, of which gauge charge is assigned to be $\psi_X(1,1,0,X)$ with the $U(1)_X$ charge X. The SM fields do not have the $U(1)_X$ charge and do not couple to the hidden sector directly. Thus, we require a mediator field between the SM and the hidden sector. We introduce an extra Higgs doublet H_1 as the mediator and as a result we have two Higgs doublets in this model. The gauge charges of the mediator H_1 and the SM Higgs doublet H_2 are assigned to be

$$H_1\left(1,2,\frac{1}{2},\frac{1}{2}\right), \qquad H_2\left(1,2,\frac{1}{2},0\right), \qquad (1)$$

under the gauge group $SU(3)_c \times SU(2)_L \times U(1)_Y \times U(1)_X$. The kinetic mixing of $U(1)_X$ with the SM $U(1)_Y$ is ignored here.

We write the Lagrangian of the Higgs sector as

$$\mathcal{L}_H = (D^\mu H_1)^\dagger D_\mu H_1 + (D^\mu H_2)^\dagger D_\mu H_2 - V(H_1, H_2) + \mathcal{L}_Y(H_2), \qquad (2)$$

where $V(H_1, H_2)$ is the Higgs potential and $\mathcal{L}_Y$ the Yukawa interactions,

$$-\mathcal{L}_Y = g_{ij}^d \bar{Q}_L^i H_2 d_R^j + g_{ij}^u \bar{Q}_L^i \tilde{H}_2 u_R^j + g_{ij}^l \bar{L}_L^i H_2 l_R^j + \text{H.c.}, \qquad (3)$$

with $\tilde{H}_2 = i\sigma_2 H^*$. The covariant derivative is written by

$$D^\mu = \partial^\mu + igW^{\mu a}T^a + ig'B^\mu Y + ig_X A_X^\mu X. \qquad (4)$$

Because of the $U(1)_X$ charge, H_1 does not couple to the SM fermions and the flavor structure of this model is naturally that of the 2HDM of type I. The Higgs potential is given by

$$V(H_1, H_2) = \mu_1^2 H_1^\dagger H_1 + \mu_2^2 H_2^\dagger H_2 + \lambda_1 (H_1^\dagger H_1)^2 + \lambda_2 (H_2^\dagger H_2)^2 + \lambda_3 (H_1^\dagger H_1)(H_2^\dagger H_2) + \lambda_4 (H_1^\dagger H_2)(H_2^\dagger H_1), \qquad (5)$$

where the soft breaking term and the λ_5 terms are prevented by the $U(1)_X$ charge.

After the EWSB, two vacuum expectation values (VEVs) are evolved,

$$H_i = \begin{pmatrix} H_i^+ \\ \frac{1}{\sqrt{2}}(v_i + \rho_i + i\eta_i) \end{pmatrix}, \qquad (6)$$

where $v_1^2 + v_2^2 = v^2$. We define the ratio $\tan\beta \equiv v_2/v_1$. The $U(1)_X$ gauge boson A_X as well as the SM gauge bosons get masses from the EWSB. Keeping the photon A as a massless mode, we find that the extra massive neutral gauge boson Z' is mixed with the ordinary Z boson to yield the physical states

$$
\begin{pmatrix} A_X \\ W^3 \\ B \end{pmatrix} = \begin{pmatrix} c_X Z' + s_X Z \\ -s_X c_W Z' + c_X c_W Z + s_W A \\ s_X s_W Z' - c_X s_W Z + c_W A \end{pmatrix}, \quad (7)
$$

where $s_X = \sin\theta_X$, $c_X = \cos\theta_X$ with the $Z - Z'$ mixing angle θ_X, and $s_W = \sin\theta_W$, $c_W = \cos\theta_W$ with the Weinberg angle θ_W. The gauge boson masses are given by

$$
m_{Z,Z'}^2 = \frac{1}{8}(g_X^2 v_1^2 + (g^2 + g'^2)v^2 \\
\pm \sqrt{(g_X^2 v_1^2 - (g^2+g'^2)v^2)^2 + 4g_X^2(g^2+g'^2)v_1^4}), \quad (8)
$$

and the mixing angle θ_X is given by

$$
\tan 2\theta_X = \frac{-2g_X\sqrt{g^2+g'^2}v^2\cos^2\beta}{(g^2+g'^2)v^2 - g_X^2 v^2\cos^2\beta}. \quad (9)
$$

Two new parameters, the $U(1)_X$ gauge coupling g_X and $\tan\beta$ are introduced in the electroweak sector. We take two observables, the dark Z mass $m_{Z'}$ and $\tan\beta$ as free parameters by translating g_X into $m_{Z'}$. Then the mixing angle can be expressed by

$$
s_X^2 = \frac{m_W^2 \cos^2\beta}{c_W^2(m_Z^2 - m_{Z'}^2) - m_W^2 \cos^2\beta} \frac{m_{Z'}^2}{m_Z^2 - m_{Z'}^2} \quad (10)
$$

in terms of observables.

We write the NC interactions in terms of the physical gauge bosons as

$$
\mathcal{L}_{NC} = -eA^\mu \bar{f}Q\gamma_\mu f - c_X Z^\mu(g_V \bar{f}\gamma_\mu f + g_A \bar{f}\gamma_\mu \gamma_5 f) \\
+ s_X Z'^\mu(g_V \bar{f}\gamma_\mu f + g_A \bar{f}\gamma_\mu\gamma_5 f), \quad (11)
$$

where the couplings e, g_V, and g_A are defined in the same manner as those of the SM. Note that the Z' couplings are the same as the ordinary Z couplings up to the suppression factor $\tan\theta_X$. Therefore, we call the extra gauge boson Z' the dark Z boson.

After the EWSB, we diagonalize the mass matrices of the neutral and charged Higgs bosons to derive physical states and to get the physical masses. We have two CP-even neutral scalar bosons of which masses are given by

$$
m_{h,H}^2 = \lambda_1 v_1^2 + \lambda_2 v_2^2 \pm \sqrt{(\lambda_1 v_1^2 - \lambda_2 v_2^2)^2 + (\lambda_3 + \lambda_4)^2 v_1^2 v_2^2}, \quad (12)
$$

and the mixing angle α is given by

$$
\tan 2\alpha = \frac{-(\lambda_3 + \lambda_4)\tan\beta}{\lambda_1 - \lambda_2 \tan^2\beta}. \quad (13)
$$

The physical states of the neutral Higgs bosons are defined by

$$
\begin{pmatrix} \rho_1 \\ \rho_2 \end{pmatrix} = \begin{pmatrix} \cos\alpha & \sin\alpha \\ -\sin\alpha & \cos\alpha \end{pmatrix} \begin{pmatrix} h \\ H \end{pmatrix} = \begin{pmatrix} h\cos\alpha + H\sin\alpha \\ -h\sin\alpha + H\cos\alpha \end{pmatrix}, \quad (14)
$$

where H is the SM-like Higgs boson and h is the extra neutral Higgs boson.

Diagonalizing the charged states, we have a pair of charged Higgs bosons $H^\pm$ of which masses are

$$
m_\pm^2 = -\frac{1}{2}\lambda_4 v^2, \quad (15)
$$

and a pair of massless modes, where the mixing angle is

$$
\tan 2\beta = \frac{2M_{12}^2}{M_{11}^2 - M_{22}^2} = \frac{2v_1 v_2}{v_1^2 - v_2^2}. \quad (16)
$$

The charged states are given in terms of $H_1^\pm$, $H_2^\pm$,

$$
\begin{pmatrix} H_1^\pm \\ H_2^\pm \end{pmatrix} = \begin{pmatrix} \cos\beta & -\sin\beta \\ \sin\beta & \cos\beta \end{pmatrix} \begin{pmatrix} G^\pm \\ H^\pm \end{pmatrix} \\
= \begin{pmatrix} G^\pm \cos\beta - H^\pm \sin\beta \\ G^\pm \sin\beta + H^\pm \cos\beta \end{pmatrix}, \quad (17)
$$

where the massless modes $G^\pm$ are corresponding to the longitudinal modes of the $W^\pm$ bosons.

III. ANALYSES

In this section, we analyze our model by considering both theoretical constraints and experimental limits. We use the following set of independent model parameters:

$$
(m_{Z'}, \sin\alpha, \tan\beta, m_h, m_\pm), \quad (18)
$$

where m_h and $m_\pm$ are defined in Eqs. (12) and (15), respectively. Manifestly, we also use the $U(1)_X$ coupling g_X and the $Z - Z'$ mixing s_X in the formulas for convenience.

A. Higgs phenomenology

There are two CP-even neutral scalar bosons and a pair of charged scalar bosons after the EWSB in this model. One neutral scalar is the SM-like Higgs boson of which mass is fixed as the measured value $m_H = 125.10$ GeV. The other neutral scalar boson may be either lighter or heavier than the SM-like Higgs boson and its mass m_h is a

free parameter of the model. The other free parameters of the Higgs sector are the charged Higgs mass $m_\pm$ and the mixing angles α and β.

In order to analyze the Higgs potential, we write the Higgs quartic couplings in terms of masses and mixing angles,

$$\lambda_1 = \frac{1}{2v_1^2}(m_h^2\cos^2\alpha + m_H^2\sin^2\alpha),$$

$$\lambda_2 = \frac{1}{2v_2^2}(m_h^2\sin^2\alpha + m_H^2\cos^2\alpha),$$

$$\lambda_3 = \frac{1}{v^2}\left(2m_\pm^2 + \frac{\sin 2\alpha}{\sin^2\beta}(m_H^2 - m_h^2)\right),$$

$$\lambda_4 = -\frac{2m_\pm^2}{v^2}. \tag{19}$$

The quartic couplings are assumed to be in the perturbative domain, $|\lambda_i| < 4\pi$ in this analysis. The potential should be bounded from below with the following conditions:

$$\lambda_1 > 0, \qquad \lambda_2 > 0, \qquad \lambda_3 > -2\sqrt{\lambda_1\lambda_2},$$

$$\lambda_3 + \lambda_4 > -2\sqrt{\lambda_1\lambda_2}, \tag{20}$$

for the stable vacuum. We also require the perturbative unitarity of the WW scattering at tree level, which is translated into the following conditions [10,11]:

$$|\lambda_1| < 4\pi, \qquad |\lambda_2| < 4\pi, \qquad |\lambda_3| < 8\pi,$$

$$|\lambda_3 + \lambda_4| < 8\pi, \qquad |\lambda_3 + 2\lambda_4| < 8\pi,$$

$$|\lambda_1 + \lambda_2 \pm \sqrt{(\lambda_1 - \lambda_2)^2 + \lambda_4^2}| < 8\pi,$$

$$|3(\lambda_1 + \lambda_2) \pm \sqrt{9(\lambda_1 - \lambda_2)^2 + (2\lambda_3 + \lambda_4)^2}| < 8\pi,$$

$$\sqrt{\frac{2\lambda_3^2 + 4\lambda_3\lambda_4 + \lambda_4^2}{2}} < 8\pi. \tag{21}$$

A lot of data from Higgs search experiments and the measurements of the SM-like Higgs boson have been provided by collider experiments, at LEP, Tevatron, and LHC. We implement the analysis to achieve allowed parameter sets of the extended Higgs sector by applying experimental limits using the public codes HiggsBounds [8], which compares various predictions in the Higgs sector with experimental data. HiggsBounds includes the exclusion limits at the 95% C.L. for the extended Higgs boson searches. We also use HiggsSignals [9], which performs a χ^2 test of the Higgs sector predictions against the signal rate and mass measurements from colliders. The code HiggsSignals computes the signal strengths with model parameters.

For HiggsBounds and HiggsSignals, we express the effective couplings κ_{ijk} in terms of model parameters given in in Eq. (18). The effective couplings are normalized by the corresponding SM couplings.

The scalar to fermion pair couplings are given by

$$\kappa_{H\bar{f}f} = \frac{\cos\alpha}{\sin\beta}, \qquad \kappa_{h\bar{f}f} = -\frac{\sin\alpha}{\sin\beta}, \tag{22}$$

where the SM couplings are $g_{H\bar{f}f} = -m_f/v$. The triple couplings of one scalar to two gauge bosons normalized by the SM Higgs couplings $g_{HWW}^{SM} = gm_W$ and $g_{HZZ}^{SM} = gm_Z/c_W$, respectively, are read as

$$\kappa_{HW^+W^-} = \sin(\alpha + \beta),$$

$$\kappa_{hW^+W^-} = \cos(\alpha + \beta), \tag{23}$$

and

$$\kappa_{HZZ} = c_X^2\sin(\alpha + \beta) - \cos\beta\sin\alpha\left(\frac{2g_X}{g}c_Wc_Xs_X - \left(\frac{g_X}{g}\right)^2c_W^2s_X^2\right),$$

$$\kappa_{hZZ} = c_X^2\cos(\alpha + \beta) - \cos\beta\cos\alpha\left(\frac{2g_X}{g}c_Wc_Xs_X - \left(\frac{g_X}{g}\right)^2c_W^2s_X^2\right),$$

$$\kappa_{HZZ'} = -c_Xs_X\sin(\alpha + \beta) - \cos\beta\sin\alpha\left(\frac{g_X}{g}c_X^2 - \frac{g_X}{g}c_Ws_X^2 - \left(\frac{g_X}{g}\right)^2c_W^2c_Xs_X\right),$$

$$\kappa_{hZZ'} = -c_Xs_X\cos(\alpha + \beta) - \cos\beta\cos\alpha\left(\frac{g_X}{g}c_X^2 - \frac{g_X}{g}c_Ws_X^2 - \left(\frac{g_X}{g}\right)^2c_W^2c_Xs_X\right),$$

$$\kappa_{HZ'Z'} = s_X^2\sin(\alpha + \beta) + \cos\beta\sin\alpha\left(\frac{2g_X}{g}c_Wc_Xs_X + \left(\frac{g_X}{g}\right)^2c_W^2c_X^2\right),$$

$$\kappa_{hZ'Z'} = s_X^2\cos(\alpha + \beta) + \cos\beta\cos\alpha\left(\frac{2g_X}{g}c_Wc_Xs_X + \left(\frac{g_X}{g}\right)^2c_W^2c_X^2\right). \tag{24}$$

We find both the SM-like Higgs boson and the additional neutral scalar boson can decay into ZZ' and $Z'Z'$ modes depending on $m_{Z'}$ and m_h, which do not exist in the typical 2HDM. These channels are open due to the $U(1)_X$ charge assignment for the H_1 as well as the mixing between the Z and Z' bosons. Thus, these decay channels must be taken into account for the calculation of the branching ratios of the scalar bosons, which are input information for the HiggsBounds and HiggsSignals. Furthermore, these channels can probe distinct signals of this model from the typical 2HDMs with discrete Z_2 symmetry as well as the SM. Actually we

find that $\mathrm{Br}(H \to Z'Z') < 1.6\%$ for the allowed parameter space and $\mathrm{Br}(H \to ZZ')$ can reach 9% to the highest. We expect that $H \to Z'Z'$ and $H \to ZZ'$ processes can be observed at the LHC in the future if the Z' boson would decay inside the detector to leave a displaced vertex.

The triple gauge couplings read as

$$\kappa_{W^+W^-Z} = c_X, \qquad \kappa_{W^+W^-Z'} = -s_X, \tag{25}$$

and the Higgs triple couplings read as

$$\begin{aligned}
\kappa_{HHH} &= 3(2\lambda_1\sin^3\alpha\cos\beta + 2\lambda_2\cos^3\alpha\sin\beta + (\lambda_3+\lambda_4)\cos\alpha\sin\alpha\cos(\alpha-\beta)), \\
\kappa_{hhh} &= 3(2\lambda_1\cos^3\alpha\cos\beta - 2\lambda_2\sin^3\alpha\sin\beta + (\lambda_3+\lambda_4)\cos\alpha\sin\alpha\cos(\alpha-\beta)), \\
\kappa_{Hhh} &= 6\cos\alpha\sin\alpha(\lambda_1\cos\alpha\cos\beta + \lambda_2\sin\alpha\sin\beta) + (\lambda_3+\lambda_4)(\sin(\alpha+\beta) - 3\cos\alpha\sin\alpha\cos(\alpha-\beta)), \\
\kappa_{HHh} &= 6\cos\alpha\sin\alpha(\lambda_1\sin\alpha\cos\beta - \lambda_2\cos\alpha\sin\beta) + (\lambda_3+\lambda_4)(\cos(\alpha+\beta) - 3\cos\alpha\sin\alpha\sin(\alpha-\beta)), \tag{26}
\end{aligned}$$

with normalization of v^2/m_Z^2. Note that the SM coupling is $g_{HHH}^{\mathrm{SM}} = 3m_H^2/v = 6\lambda v$.

Since there are no charged Higgs bosons in the SM, the effective couplings with the charged Higgs bosons are defined by appropriate normalizations. The charged Higgs to fermion couplings are given by

$$\kappa_{H^\pm \bar{f}f} = \frac{1}{\tan\beta}, \tag{27}$$

with the normalization $\sqrt{2}m_f/v$. We write the couplings of the charged Higgs bosons to neutral gauge bosons as

$$g_{ZH^\pm H^\mp} = \frac{1}{c_W}\left((1-2s_W^2)c_X + \frac{g_X}{g}c_W s_X \sin^2\beta\right),$$

$$g_{Z'H^\pm H^\mp} = \frac{1}{c_W}\left(-(1-2s_W^2)s_X + \frac{g_X}{g}c_W c_X \sin^2\beta\right) \tag{28}$$

without normalization. Note that $g_{ZH^\pm H^\mp} = (1-2s_W^2)/c_W$ in the typical 2HDM. The neutral and charged Higgs couplings associated with the $W^\pm$ boson are given by

$$\begin{aligned}
\kappa_{HH^\pm W^\mp} &= \cos(\alpha+\beta), \\
\kappa_{hH^\pm W^\mp} &= -\sin(\alpha+\beta), \tag{29}
\end{aligned}$$

and the neutral and charged gauge boson couplings associated with the $H^\pm$ are given by

$$\begin{aligned}
\kappa_{ZH^\pm W^\mp} &= -\left(\frac{g_X}{g}\right)\cos\beta\sin\beta c_W s_X, \\
\kappa_{Z'H^\pm W^\mp} &= -\left(\frac{g_X}{g}\right)\cos\beta\sin\beta c_W c_X. \tag{30}
\end{aligned}$$

The Higgs triple couplings with the charged Higgs boson are

$$\begin{aligned}
\kappa_{HH^+H^-} &= 2\lambda_1\sin\alpha\cos\beta\sin^2\beta + 2\lambda_2\cos\alpha\sin\beta\cos^2\beta + \lambda_3(\cos\alpha\sin^3\beta + \sin\alpha\cos^3\beta) \\
&\quad - \lambda_4(\cos\alpha\cos^2\beta\sin\beta + \sin\alpha\cos\beta\sin^2\beta), \\
\kappa_{hH^+H^-} &= 2\lambda_1\cos\alpha\cos\beta\sin^2\beta - 2\lambda_2\sin\alpha\sin\beta\cos^2\beta + \lambda_3(\cos\alpha\cos^3\beta - \sin\alpha\sin^3\beta) \\
&\quad + \lambda_4(\sin\alpha\cos^2\beta\sin\beta - \cos\alpha\cos\beta\sin^2\beta) \tag{31}
\end{aligned}$$

with normalization of v^2/m_Z^2.

We require that randomly generated free parameters of (18) have to pass the exclusion limit of HiggsBounds and then the P value evaluated from HiggsSignals is less than 0.05.

B. $\Delta\rho$ constraints

In this model, the Z boson mass is shifted by the Z' boson mass,

$$m_Z^2 = \frac{m_W^2}{c_W^2 c_X^2} - m_{Z'}^2 \frac{s_X^2}{c_X^2}, \tag{32}$$

at tree level, while the $W^{\pm}$ mass remains unchanged. Thus, the ρ parameter defined by the ratio of W and Z boson masses $\rho \equiv m_W^2/m_Z^2 c_W^2$ should be modified. The correction $\Delta\rho_X$ parametrizes the NP effects,

$$\Delta\rho_X \equiv 1 - \frac{1}{\rho} \approx -s_X^2\left(1 - \frac{m_{Z'}^2 c_W^2}{m_W^2}\right), \tag{33}$$

in the leading order of s_X.

There also exist new scalar contributions to the ρ parameter $\Delta\rho_H$ at loop levels. We calculate $\Delta\rho_H$ in our model such that [12]

$$\begin{aligned}\Delta\rho_H = &\frac{\alpha}{16\pi^2 m_W^2 s_W^2}(\sin^2(\alpha+\beta)F(m_\pm^2,m_H^2)\\ &+ \cos^2(\alpha+\beta)F(m_\pm^2,m_h^2) + 3\cos^2(\alpha+\beta)F(m_{Z'}^2,m_H^2)\\ &+ 3\sin^2(\alpha+\beta)F(m_{Z'}^2,m_h^2) - 3\cos^2(\alpha+\beta)F(m_W^2,m_H^2)\\ &- 3\sin^2(\alpha+\beta)F(m_W^2,m_h^2)),\end{aligned} \tag{34}$$

where

$$F(x,y) = \frac{x+y}{2} - \frac{xy}{x-y}\ln\frac{x}{y}. \tag{35}$$

Generically, the Higgs loop contributions to $\Delta\rho$ vanish when we take a limit of custodial symmetry in the 2HDM. However, our model assigns the $U(1)_X$ gauge symmetry only to H_1, which leads to $\lambda_5 = 0$ in the Higgs potential and the explicit violation of the custodial symmetry. Thus, the custodial symmetry limit is derived in this model only when we put $\lambda_4 = 0$, which results in $m_\pm = 0$.

The NP correction $\Delta\rho = \Delta\rho_X + \Delta\rho_H$ is constrained by the experimental value of $\Delta\rho$. It is obtained from the T variable by the relation

$$\Delta\rho = \alpha(m_Z)T. \tag{36}$$

The measured T value and the fine-structure constant are given by

$$T = 0.09 \pm 0.07,$$
$$\alpha^{(5)}(m_Z)^{-1} = 127.955 \pm 0.010, \tag{37}$$

from PDG [13], where the superscript (5) denotes the five-loop result in QED.

C. The atomic parity violation

The precise measurement of the atomic parity violation (APV) in the atomic spectra constrains the NP effects in the NC interaction. The effective Lagrangian for the APV is written as

$$\mathcal{L} = -\frac{G_F}{\sqrt{2}}(g_{AV}^u(\bar{e}\gamma_\mu\gamma^5 e)(\bar{u}\gamma^\mu u) + g_{AV}^d(\bar{e}\gamma_\mu\gamma^5 e)(\bar{d}\gamma^\mu d)), \tag{38}$$

where the nucleon couplings $g_{AV}^p \equiv 2g_{AV}^u + g_{AV}^d$ and $g_{AV}^n \equiv g_{AV}^u + 2g_{AV}^d$. We define the weak charge of the nuclei

$$Q_W \equiv -2(Zg_{AV}^p + Ng_{AV}^n), \tag{39}$$

where Z (N) is the number of protons (neutrons) in the atom. The weak charge $Q_W^{SM} \approx -N + Z(1 - 4s_W^2)$ at tree level in the SM.

Including the dark Z contribution, we have

$$Q_W = Q_W^{SM}\left(1 + \frac{m_Z^2}{m_{Z'}^2}s_X^2\right), \tag{40}$$

in the leading order of s_X. Using the SM value $Q_W^{SM} = -73.16 \pm 0.03$ [14,15] and the present experimental value for the Cs atom [16]

$$Q_W^{exp} = -72.82 \pm 0.42, \tag{41}$$

we achieve the constraint on the model

$$\frac{m_Z^2}{m_{Z'}^2}s_X^2 \le 0.006, \tag{42}$$

at 95% C.L.

D. Z boson decays

The dark Z boson and the additional neutral Higgs h might be light in this model. When the sum of the masses of the dark Z and h is less than the Z boson mass, the $Z \to Z'h$ channel opens and it contributes to the Z boson total width. The width of $Z \to Z'h$ decay is given by

$$\begin{aligned}\Gamma(Z \to Z'h) = &\frac{g^2\kappa_{hZZ'}^2}{192\pi m_Z c_W^2 m_{Z'}^2}(m_h^4 - 2m_h^2 m_Z^2 - 2m_h^2 m_{Z'}^2\\ &+ m_Z^4 + 10m_Z^2 m_{Z'}^2 + m_{Z'}^4)\\ &\times\left(1 - \frac{2m_h^2}{m_Z^2} - \frac{2m_{Z'}^2}{m_Z^2} + \frac{m_h^4}{m_Z^4} + \frac{m_{Z'}^4}{m_Z^4} - \frac{2m_h^2 m_{Z'}^2}{m_Z^4}\right).\end{aligned} \tag{43}$$

The dark Z decays are suppressed by the $Z - Z'$ mixing $\sin\theta_X$ and the h decays suppressed by $\sin\alpha$. Then the Z'

and h live long and decay outside the detector when the DM particle mass is larger than half the Z' mass. If the DM particle is light enough, the Z' will decay into a pair of the DM particles. Eventually the $Z \to Z'h$ decay will contribute to the invisible Z decay width in most cases.

We add the partial width of $Z \to Z'h$ decay to the SM total width, $\Gamma_Z^{\mathrm{New}} = \Gamma_Z^{\mathrm{SM}} + \Gamma(Z \to Z'h)$, and constrain the model prediction by the experimental limits. The Z total width Γ_Z is precisely measured at LEP and SLD [17],

$$\Gamma_Z = 2.4955 \pm 0.0023 \text{ GeV} \qquad (44)$$

and shows a good agreement with the SM prediction $\Gamma_Z^{\mathrm{SM}} = 2.4941 \pm 0.0009$ GeV. Since Γ_Z is very precisely measured, the additional contribution $\Gamma(Z \to Z'h)$ should be highly suppressed.

E. Results

Figure 1 depicts the parameter set $(m_{Z'}, |\sin \theta_X|)$ allowed by the HiggsBounds, HiggsSignals, and the electroweak constraints. We find that the very light Z' is possible if the mixing angle is small enough. Such a light and feebly interacting Z' will be probed in the future intensity frontier experiments and long-lived particle searches.

We see that there are two regions in the parameter space, the light dark Z region, $m_{Z'} < 12$ GeV, and the heavy region, $m_{Z'} > 30$ GeV. The reason why there are two separate regions of allowed parameters is that each region corresponds to different suppression conditions of the $Z \to Z'h$ decay. The light dark Z region corresponds to the small mixing angle $|s_X|$ and, consequently, the suppressed coupling of $\kappa_{hZZ'}$, while the heavy region corresponds to

the kinematic suppression. The kinematic suppression implies either $m_Z \approx m_{Z'} + m_h$ or $m_Z < m_{Z'} + m_h$. If $m_Z < m_{Z'} + m_h$, the decay channel does not open and no constraints come from the Z total width. When $m_Z \approx m_{Z'} + m_h$, although the decay channel opens, $\Gamma(Z \to Z'h)$ is suppressed by the smallness of the kinematic factor, which is factorized by $(m_Z - m_{Z'} - m_h)$.

Separation of parameter sets is clearly demonstrated in Fig. 2. The values of $\tan \beta$ and m_h are crucially constrained in the light dark Z region. We find that $13 < \tan \beta < 15$ and $50 < m_h < 55$ GeV when $m_{Z'} < 12$ GeV. On the other hand, in the case of kinematic suppression, a wide range of parameters is allowed. We see that $13 < \tan \beta < 42$ and $10 < m_h < 55$ GeV when $m_{Z'} > 30$ GeV.

The allowed masses and mixing angles of the additional neutral Higgs boson and the charged Higgs bosons are shown in Fig. 3. The allowed mass of h is $10 < m_h < 55$ GeV as also shown in Fig. 2. We see that the small mixing angle is preferred, $|\sin \alpha| < 0.004$, which implies that the fermion-coupled scalar ρ_2 is mostly the SM-like Higgs boson H. Consequently, the VEVs $v_2 \sim v$, $\tan \beta$ is expected to be large and the additional scalar is generically lighter than the SM-like Higgs boson. Since $\tan \beta$ is large enough, the model is free from constraints from the $b \to s\gamma$ decays in B physics and $H^\pm \to \tau\nu$ and $H^\pm \to tb$ decays at the LHC. We can see that there are also two groups of allowed points in $(m_h, \sin \alpha)$ and $(m_\pm, \tan \beta)$ planes, which are corresponding to the coupling suppression and the kinematic suppression for $Z \to Z'h$ decay, respectively, as explained above.

Before moving to the DM phenomenology, we emphasize that our model is still viable as one of the simplest extensions of the SM, even without the hidden sector.
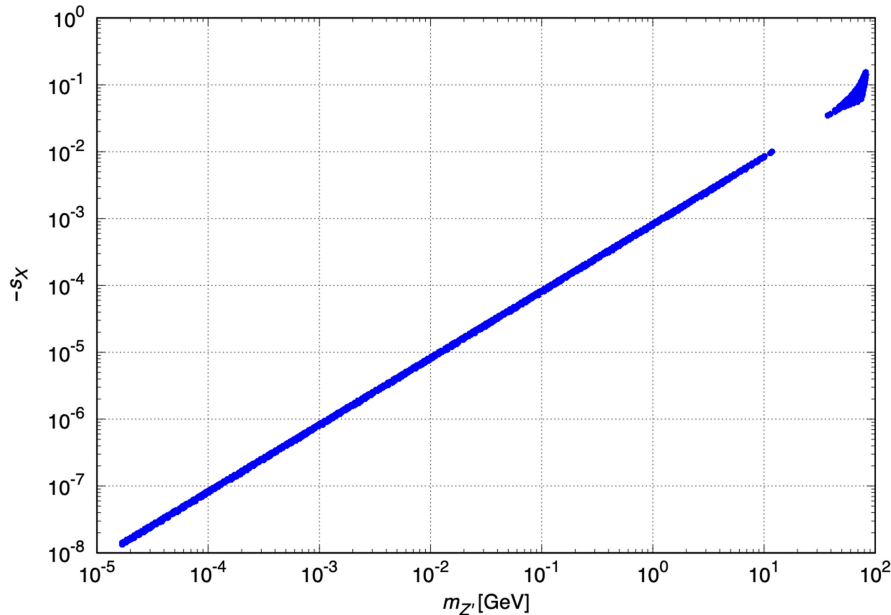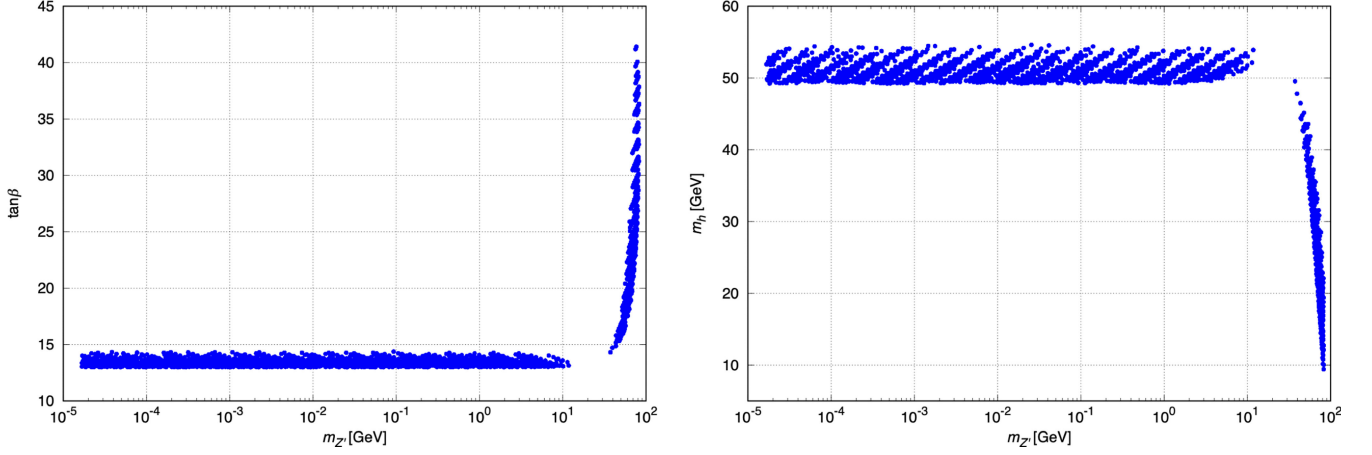

FIG. 1. Allowed parameter set of $(m_{Z'}, |\sin \theta_X|)$.

FIG. 2. Allowed values of $\tan\beta$ (left) and m_h (right) with respect to $m_{Z'}$.

We should mention that the Z boson decay width in this section does not include the decay channels into hidden sector particles. Depending on the configuration of the hidden sector, the Z boson decay width could further constrain the parameter space.

IV. DARK MATTER PHENOMENOLOGY

We introduce a vectorlike Dirac fermion with $\mathrm{U}(1)_X$ gauge symmetry in the hidden sector, which is a candidate for DM. The hidden sector Lagrangian is given by

$$\mathcal{L}_{\mathrm{hs}} = -\frac{1}{4} F_X^{\mu\nu} F_{X\mu\nu} + \bar{\psi}_X i\gamma^\mu D_\mu \psi_X - m_X \bar{\psi}_X \psi_X, \quad (45)$$

where

$$D_\mu = \partial_\mu + ig_X A_\mu^X X \quad (46)$$

with X and m_X being the $\mathrm{U}(1)_X$ charge and the mass for the ψ_X, respectively. As a result of the spontaneous

symmetry breaking and consequential $Z - Z'$ mixing, the DM interaction terms with the physical gauge bosons are reformulated as

$$\mathcal{L}_{\mathrm{DM}}^{\mathrm{int}} = ig_X X \bar{\psi}_X \gamma^\mu \psi_X (c_X Z'_\mu + s_X Z_\mu). \quad (47)$$

Note that we have only two additional parameters, m_X and X, which are independent of the structure of the visible sector. Based on the Dirac fermionic DM scenario, we perform the phenomenological analysis on properties of DM with microOMEGAs [18], especially for the relic abundance and the DM-nucleon cross section for the allowed values of parameters in the previous section. A thermal freeze-out scenario is assumed for the relic abundance calculation.

The most recent DM contribution to the relic abundance density Ω is obtained from measurements of the anisotropy of the cosmic microwave background and of the spatial distribution of galaxies [19]. The present value of the relic density for nonbaryonic cold DM (CDM) is
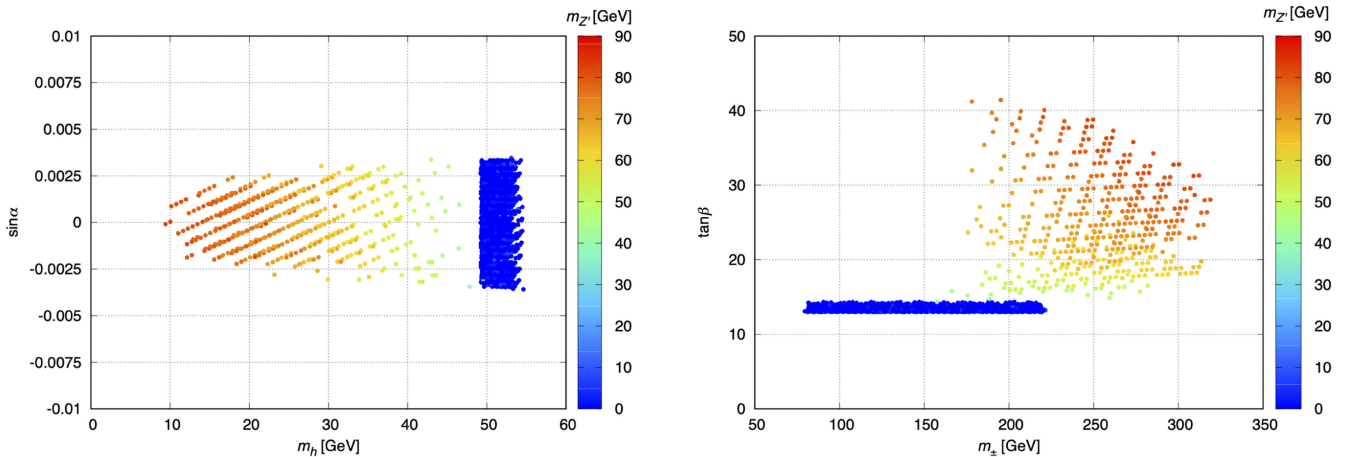
FIG. 3. Allowed parameter set of $(m_h, \sin\alpha)$ (left) and $(m_\pm, \tan\beta)$ (right).
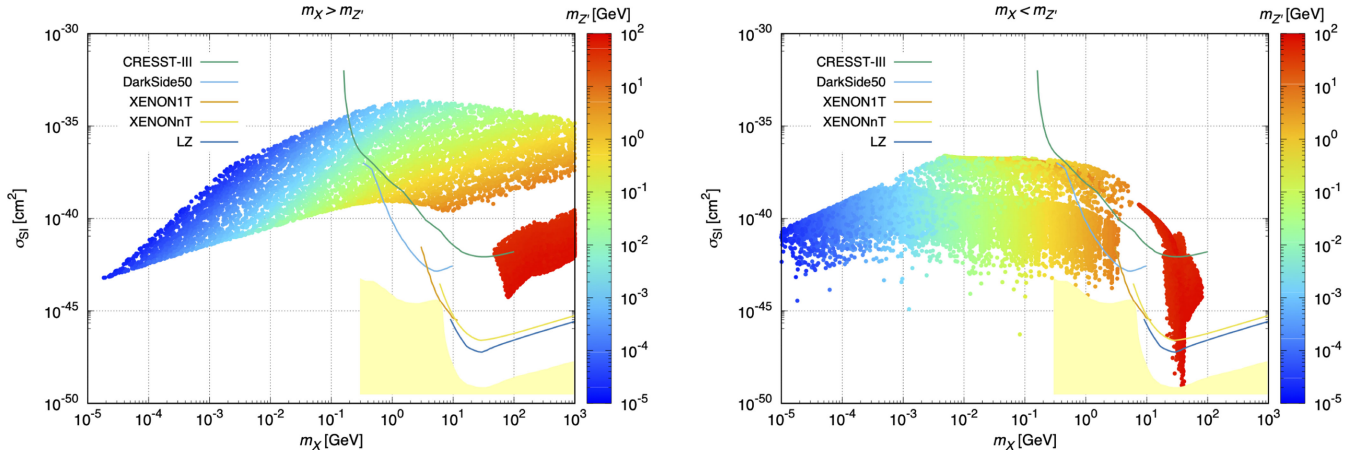
FIG. 4.   Results of the DM-nucleon cross sections for $m_X > m_{Z'}$ (left) and $m_X < m_{Z'}$ (right). Discovery bounds from various direct detection limits are shown together. The yellow shaded region is the neutrino background.

$$\Omega_{\mathrm{CDM}} h^2 = 0.120 \pm 0.001. \qquad (48)$$

Such a precise value provides a stringent constraint on the model parameters. We search for the parameter sets of the DM mass and its charge X that make the relic abundance stay within 3-σ range from the central value of the observation, with the perturbativity constraint $g_X X \leq \sqrt{4\pi}$. The acceptable relic density can be achieved mainly through the DM annihilation processes such as $\psi_X \bar{\psi}_X \to Z' \to$ SM particles, $\psi_X \bar{\psi}_X \to Z'Z'$, and the Higgsstrahlung $\psi_X \bar{\psi}_X \to Z'h$ depending on the mass spectra.

In Fig. 4, we show the DM-nucleon cross sections for the parameter sets that are consistent with the observed relic density within 3-σ range. We also apply the constraint from the total decay width of the Z boson, which can be modified by the new decay channel $Z \to \psi_X \bar{\psi}_X$. The parameter sets that give rise to too large DM self-interaction are excluded by imposing the "bullet cluster" constraint, $\sigma/m_{\mathrm{DM}} \lesssim 1$ cm^2/g [20]. As a result, the allowed mass range for the Z' boson is slightly further constrained as $m_{Z'} \lesssim 7$ and $43 \lesssim m_{Z'} \lesssim 83$ GeV, compared with the result in the previous section which is analyzed without specifying the DM properties.

The left figure in Fig. 4 represents the case that the DM fermion is heavier than Z', $m_X > m_{Z'}$. The experimental bounds from CRESST III [21], XENON1T [22], XENONnT [23], DarkSide-50 [24], and LZ [25] are shown together. In this case, the high mass region for the DM fermion is excluded by various direct detection experiments and the DM mass is limited below a few hundred MeV. Accordingly, relatively large Z' mass is prohibited and low mass for Z', less than about a few hundred MeV, is preferred.

On the other hand, the right figure in Fig. 4 provides the results for $m_X < m_{Z'}$. In this case, a resonance can be possible in the DM annihilation process $\psi_X \bar{\psi}_X \to Z' \to$ SM

when $2m_X \sim m_{Z'}$ and the DM pair annihilation rate during the freeze-out is enhanced. This enhancement requires the strength of the couplings to be smaller than those for nonresonance cases to fit the observed relic density. Consequently, the DM-nucleon cross section becomes smaller under the resonance condition and more points survive the limits from the direct detection experiments compared with the previous case of $m_X > m_{Z'}$. For example, the dip around $m_X \sim 40$ GeV survives the LZ limit for the DM direct detection. In this region, we have "double" resonances such as $2m_X \sim m_{Z'} \sim m_Z$ and the DM-nucleon cross section is suppressed by cancellation between the two diagrams with Z and Z' exchange, respectively.

Since light DM is favored in our model, we should consider electron-recoil experiments for DM direct detection. We estimate the cross sections following Ref. [26], and it turns out that the cross sections survive the limits put by many experiments. However, the values of the cross sections are small and it is unlikely that the signals from the electron-recoil experiments would be detected in the near future. The results together with experimental limits from EDELWEISS [27], DAMIC [28], SENSEI [29], PandaX-II [30], and XENON1T [31] are shown in Fig. 5.

In Fig. 6, we show the parameter sets in the $(m_X, m_{Z'})$ plane that are consistent with the observed values of relic density, the DM self-interaction cross section bound from the bullet cluster, total decay width of the Z boson, and nonobservation of DM in the various direct detection experiments. The DM mass is highly constrained and it would be even below 1 GeV if we ignore the sharp resonance regions. It is quite interesting that the seemingly independent dark sector gives further constraint on the Z' properties. It turns out that the Z' mass of a few tenths of GeV is unfavorable except for the double resonance region of $2m_X \sim m_{Z'} \sim m_Z$, while the relatively light Z' boson below a few MeV is preferred. In consequence, the light Z'
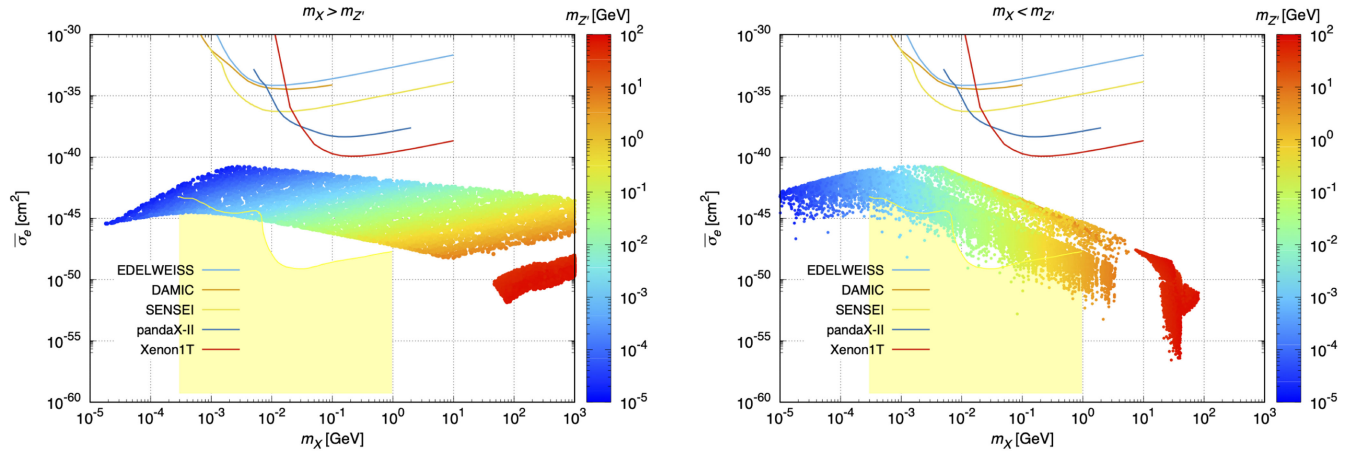
FIG. 5. Results of the electron-recoil cross sections from DM for $m_X > m_{Z'}$ (left) and $m_X < m_{Z'}$ (right). Discovery bounds from various direct detection limits are shown together. The yellow shaded region is the neutrino background.

and DM is quite natural in our model and such properties can be tested in the future collider experiments.

A few comments are in order. First, it is known that for the DM particle as light as below 1 MeV, the conventional freeze-out mechanism fails [32–34]. However, alternative cosmological scenarios are suggested that can alleviate the problems of sub-MeV DM (see, for example, Refs. [35,36]). As an another alternative, a freeze-in mechanism can be considered [37]. Second, the production of energetic particles due to self-annihilation of the DM particles in high DM density regions like the Galactic Center can give a serious constraint on the model. We evaluate the velocity-weighted annihilation cross sections $\langle \sigma v \rangle$ especially to $\tau^- \tau^+$ and $b\bar{b}$
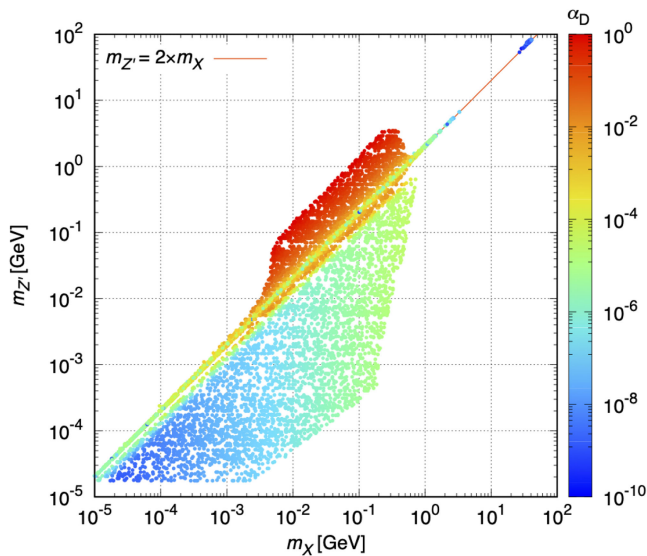

FIG. 6. Solution points in $(m_X, m_{Z'})$ plane that survive the discovery limits from the direct detection experiments. The points aligned along the red line represent the resonance points, i.e., $m_{Z'} = 2m_X$. The values of the dark fine-structure constant $\alpha_D \equiv \frac{(g_X X)^2}{4\pi}$ are presented as color contour.

since they give the most stringent constraints. We find that all the parameter sets in Fig. 6 give $\langle \sigma v \rangle \sim 10^{-33} - 10^{-26}$ cm^3 s^{-1} for both $\tau^- \tau^+$ and $b\bar{b}$ channels and most of them stay well below the constraint given by Fermi-LAT, which is $\langle \sigma v \rangle_{bb,\tau\tau} \sim 10^{-26}$ or 10^{-27} cm^3 s^{-1} for small DM masses around 2–5 GeV [38] except for few points that are severely fine-tuned through resonances. Finally, sub-GeV dark sectors can be constrained from the supernova cooling. We follow the recent comprehensive analysis of Ref. [39], where the authors draw the conclusion that even very tiny self-interaction of the DM particles can trap the DM particles inside the supernova and as a result evade the constraints from the energy luminosity of dark emission. We evaluate $\alpha_D \equiv \frac{(g_X X)^2}{4\pi}$ and $\epsilon \sim \sin \theta_X$ up to $\mathcal{O}(1)$ factor for the DM mass range 1 MeV $\sim$ 1 GeV and compare the results especially with Fig. 4 in Ref. [39]. We find that our solution points largely stay outside the exclusion region, which means that the DM trap mechanism works well and the points in Fig. 6 can circumvent the constraints from the supernova.

V. CONCLUDING REMARKS

In this work, we studied the hidden sector model connected to the SM through the dark Z boson. Since the additional SU(2)$_L$ scalar doublet with hidden U(1)$_X$ charge mediates between the hidden sector and the SM sector, the EWSB also breaks the hidden sector U(1) symmetry and generates the massive dark Z boson. Because of the hidden U(1)$_X$ charge, the additional scalar doublet does not couple to the SM fermions, and the Higgs sector structures of our model and the 2HDM of type I are alike. The *CP*-odd scalar is eaten up by the massive dark Z boson and is absent in the Higgs contents of the model. Instead, there are new couplings of the Higgs boson to the dark Z boson. We explore the Higgs phenomenology of this model using the public programs HiggsBounds and HiggsSignals. The present experimental limits to search the NP in the

Higgs sector strongly constrain the model parameter space together with the electroweak constraints.

We find that our parameter set can satisfy the relic abundance and the direct detection limits of the DM-nucleon cross section assuming that the hidden sector fermion is a DM candidate. Part of the parameter region is more excluded by the present direct detection experiments. The direct detection by the DM-electron scattering is also considered and we see that the present measurements do not affect our model. Finally, the bullet cluster, the DM annihilation at the Galactic Center, and supernova cooling constraints on the DM self-interaction are discussed to conclude that our model is safe on the whole.

[1] G. Aad *et al.* (ATLAS Collaboration), Phys. Lett. B **716**, 1 (2012).

[2] S. Chatrchyan *et al.* (CMS Collaboration), Phys. Lett. B **716**, 30 (2012).

[3] G. Bertone, D. Hooper, and J. Silk, Phys. Rep. **405**, 279 (2005).

[4] D. W. Jung, S. H. Nam, C. Yu, Y. G. Kim, and K. Y. Lee, Eur. Phys. J. C **80**, 513 (2020).

[5] D. W. Jung, K. Y. Lee, and C. Yu, Phys. Rev. D **105**, 095023 (2022).

[6] H. Davoudiasl, H. S. Lee, and W. J. Marciano, Phys. Rev. D **85**, 115019 (2012); Phys. Rev. Lett. **109**, 031802 (2012); Phys. Rev. D **89**, 095006 (2014); **92**, 055005 (2015); P. Fayet, Phys. Rev. D **103**, 035034 (2021); P. Giffin, I. M. Lewis, and Y. J. Zheng, J. Phys. G **49**, 015003 (2022); **49**, 015003 (2022).

[7] P. Ko, Y. Omura, and C. Yu, Phys. Lett. B **717**, 202 (2012); J. High Energy Phys. 01 (2014) 016.

[8] P. Bechtle, D. Dercks, S. Heinemeyer, T. Klingl, T. Stefaniak, G. Weiglein, and J. Wittbrodt, Eur. Phys. J. C **80**, 1211 (2020); P. Bechtle, O. Brein, S. Heinemeyer, O. Stål, T. Stefaniak, G. Weiglein, and K. E. Williams, Eur. Phys. J. C **74**, 2693 (2014).

[9] P. Bechtle, S. Heinemeyer, T. Klingl, T. Stefaniak, G. Weiglein, and J. Wittbrodt, Eur. Phys. J. C **81**, 145 (2021); P. Bechtle, S. Heinemeyer, O. Stål, T. Stefaniak, and G. Weiglein, Eur. Phys. J. C **74**, 2711 (2014).

[10] B. W. Lee, C. Quigg, and H. B. Thacker, Phys. Rev. D **16**, 1519 (1977).

[11] M. Muhlleitner, M. O. P. Sampaio, R. Santos, and J. Wittbrodt, J. High Energy Phys. 03 (2017) 094.

[12] W. Grimus, L. Lavoura, O. M. Ogreid, and P. Osland, J. Phys. G **35**, 075001 (2008).

[13] R. L. Workman *et al.* (Particle Data Group Collaboration), Prog. Theor. Exp. Phys. **2022**, 083C01 (2022).

[14] W. J. Marciano and A. Sirlin, Phys. Rev. D **27**, 552 (1983); **29**, 75 (1984); **31**, 213(E) (1985).

[15] W. J. Marciano and J. L. Rosner, Phys. Rev. Lett. **65**, 2963 (1990); **68**, 898(E) (1992).

[16] S. G. Porsev, K. Beloy, and A. Derevianko, Phys. Rev. D **82**, 036008 (2010); Phys. Rev. Lett. **102**, 181601 (2009).

[17] S. Schael *et al.* (ALEPH, DELPHI, L3, OPAL, SLD, LEP Electroweak Working Group, SLD Electroweak Group and SLD Heavy Flavour Group Collaborations), Phys. Rep. **427**, 257 (2006).

[18] G. Blanger, F. Boudjema, A. Goudelis, A. Pukhov, and B. Zaldivar, Comput. Phys. Commun. **231**, 173 (2018).

[19] N. Aghanim *et al.* (Planck Collaboration), Astron. Astrophys. **641**, A6 (2020); **652**, C4(E) (2021).

[20] S. W. Randall, M. Markevitch, D. Clowe, A. H. Gonzalez, and M. Bradac, Astrophys. J. **679**, 1173 (2008).

[21] A. H. Abdelhameed *et al.* (CRESST Collaboration), Phys. Rev. D **100**, 102002 (2019).

[22] E. Aprile *et al.* (XENON Collaboration), Phys. Rev. Lett. **126**, 091301 (2021).

[23] E. Aprile *et al.* (XENON Collaboration), Phys. Rev. Lett. **131**, 041003 (2023).

[24] P. Agnes *et al.* (DarkSide Collaboration), Phys. Rev. Lett. **130**, 101001 (2023).

[25] J. Aalbers *et al.* (LZ Collaboration), Phys. Rev. Lett. **131**, 041002 (2023).

[26] R. Essig, J. Mardon, and T. Volansky, Phys. Rev. D **85**, 076007 (2012).

[27] Q. Arnaud *et al.* (EDELWEISS Collaboration), Phys. Rev. Lett. **125**, 141301 (2020).

[28] A. Aguilar-Arevalo *et al.* (DAMIC Collaboration), Phys. Rev. Lett. **123**, 181802 (2019).

[29] L. Barak *et al.* (SENSEI Collaboration), Phys. Rev. Lett. **125**, 171802 (2020).

[30] C. Cheng *et al.* (PandaX-II Collaboration), Phys. Rev. Lett. **126**, 211803 (2021).

[31] E. Aprile *et al.* (XENON Collaboration), Phys. Rev. Lett. **123**, 251801 (2019).

[32] C. Boehm, M. J. Dolan, and C. McCabe, J. Cosmol. Astropart. Phys. 08 (2013) 041.

[33] D. Green and S. Rajendran, J. High Energy Phys. 10 (2017) 013.

[34] N. Sabti, J. Alvey, M. Escudero, M. Fairbairn, and D. Blas, J. Cosmol. Astropart. Phys. 01 (2020) 004.

[35] A. Berlin and N. Blinov, Phys. Rev. Lett. **120,** 021801 (2018).

[36] A. Berlin and N. Blinov, Phys. Rev. D **99,** 095030 (2019).

[37] K. J. Bae, J. O. Gong, D. W. Jung, K. Y. Lee, and C. Yu (to be published).

[38] M. Ackermann *et al.* (Fermi-LAT Collaboration), Phys. Rev. Lett. **115,** 231301 (2015).

[39] A. Sung, G. Guo, and M. R. Wu, Phys. Rev. D **103,** 103005 (2021).